

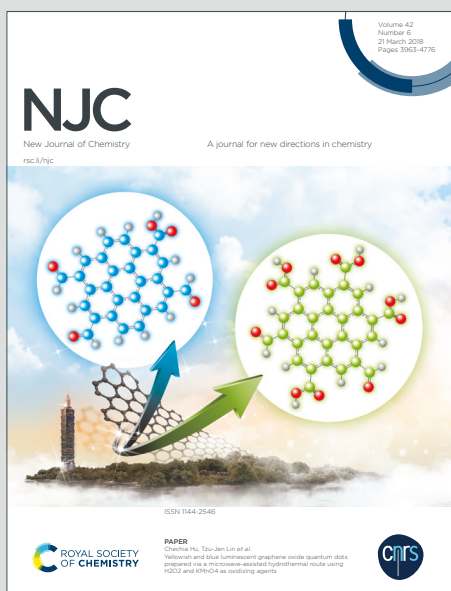
NJC

New Journal of Chemistry

Accepted Manuscript

A journal for new directions in chemistry

This article can be cited before page numbers have been issued, to do this please use: M. J. Kang, H. J. Yu, H. S. Kim and H. G. Cha, *New J. Chem.*, 2020, DOI: 10.1039/D0NJ01426E.



This is an Accepted Manuscript, which has been through the Royal Society of Chemistry peer review process and has been accepted for publication.

Accepted Manuscripts are published online shortly after acceptance, before technical editing, formatting and proof reading. Using this free service, authors can make their results available to the community, in citable form, before we publish the edited article. We will replace this Accepted Manuscript with the edited and formatted Advance Article as soon as it is available.

You can find more information about Accepted Manuscripts in the [Information for Authors](#).

Please note that technical editing may introduce minor changes to the text and/or graphics, which may alter content. The journal's standard [Terms & Conditions](#) and the [Ethical guidelines](#) still apply. In no event shall the Royal Society of Chemistry be held responsible for any errors or omissions in this Accepted Manuscript or any consequences arising from the use of any information it contains.

ARTICLE

Deep Eutectic Solvent Stabilised Co-P film for Electrocatalytic Oxidation of 5-hydroxymethylfurfural into 2,5-furandicarboxylic Acid

66 Received 00th January 20xx
Accepted 00th January 20xx

DOI: 10.1039/x0xx00000x

Myung Jong Kang,^a Hye Jin Yu,^{a,b} Hyun Sung Kim^{b,*} and Hyun Gil Cha^{a,*}

The electrocatalytic oxidation of 5-hydroxymethylfurfural (HMF) into 2,5-furandicarboxylic acid (FDCA) has been studied extensively. However, the short lifetime of catalytic electrodes remains a challenge for the electrocatalytic HMF oxidation reaction, and the high pH of the electrolyte causes denaturation of HMF during reaction. Herein, deep eutectic solvents (DES) employed in the preparation of efficient and durable catalytic electrodes for HMF oxidation. The catalytic electrode made in DES avoided the complexity of multiple alkylations, giving 99% HMF conversion and 85.3% of FDCA yield obtained with high durability, due in part to the lower pH of the electrolyte.

Introduction

Deep eutectic solvents (DES), developed by Abbot et al., consist of two or more interacting components linked by hydrogen bonding, which results in a mixture with a lower melting point than the individual precursor components.¹⁻³ DES are non-toxic, low cost, and stable against moisture compared to many known ionic liquids. DES have several superior properties such as ease of preparation, availability at fairly low cost, biodegradability with relatively low toxicity, and even be recycled more easily than pristine traditional solvents. Therefore, DES have been shown to be useful for the electrodeposition of metals and alloys such as cobalt, nickel, zinc, and tin.⁴⁻⁶ As an alternatives for traditional solvent system, usage of DES systems has been investigated in various fields such as material preparation, metal electrodeposition, solvent extraction, and lignocellulose pre-treatment.⁷⁻⁹ Recently, an efficient approaches on synthesizing DES for quaternary ammonium salts (i.e., choline chloride) and hydrogen bond donors (i.e., ethylene glycol and urea) was developed using twin screw extrusion or ball milling, which makes it possible to extend DES applications to industrial scale.^{10, 11}

Biomass is the only accessible and renewable nonfossil-based carbon source, whose utilisation will not alter the current balance of the carbon in ecosystem as biomass stores contemporary carbon.^{12, 13} One of the most attractive building block chemicals is 2,5-furandicarboxylic acid (FDCA), which produced from 5-hydroxymethylfurfural (HMF). FDCA is a

monomer that can be used for the synthesis of bio-based polymers such as polyamides, polyesters, and polyurethanes.¹⁴ For this reason, FDCA has been rated as one of the top twelve value-added chemicals by the U.S. Department of Energy (DOE).¹⁵

Till date, most reported strategies for the conversion of HMF into FDCA require harsh conditions, demanding high energy and costly production, such as high O₂ or air pressure, toxic chemical oxidants, and elevated temperature with expensive catalytic materials.^{16, 17} In this manner, the electrochemical oxidation of HMF into FDCA, which driven by electrochemical potential applied to an electrode, is an emerging approach with the advantage of eliminating O₂ or other chemical oxidants during the reaction.¹⁸⁻²⁰ Additionally, it can offer ideal conditions for HMF oxidation into FDCA by utilising noble metal-based catalysts such as Pt, Au, Pd and to reduce expenses, Co, Ni or bimetallic alloys and metal oxides/hydroxides are also used frequently.²¹⁻²³ Cu is also used frequently, however, using transition metal like Cu, Co and Ni as an electrocatalysts has huge drawback that it easily oxidise into metal oxide in alkaline conditions for HMF oxidation.²⁴ To prevent it, homo/hetero junction between transition metal and metal oxides electrodes applied in electrochemical HMF oxidation reaction, leading oxygen vacancy formation on the surface of metal oxide for better catalytic properties.²⁵⁻²⁷ Furthermore, electrochemical oxidation can be performed at ambient temperature and pressure. Despite these advantages, most of the reported results rely on noble metal catalysts in a highly basic solution, such as 1 M KOH or NaOH.^{28, 29} It is difficult to find a suitable milder electrolyte for HMF oxidation because basic conditions are required to oxidise the 2-position aldehyde group and activate the 5-position alcohol in HMF during its oxidation into FDCA.³⁰

However, an excessive amount of bases can be detrimental for HMF over a long reaction time. For example, a recent study reported by Strasser and co-workers on HMF oxidation by an

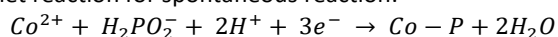
^a Center for Bio-based chemistry, Korea Research Institute of Chemical Technology (KRICT), Ulsan 44429, Republic of Korea. E-mail: hgcha@kRICT.re.kr

^b Department of Chemistry, Pukyong National University, Busan 48513, Republic of Korea.

* Electronic Supplementary Information (ESI) available: Cyclic voltammetry curves during electrodeposition, LSV curves on different concentration of P precursor, SEM images of electrodes after reaction. See DOI: 10.1039/x0xx00000x

electrochemical method using a Pt electrode in a pH 10 aqueous solution. They found that a fraction of the HMF was converted into 2,5-diformylfuran (DFF), while the very less conversion of HMF into FDCA.³¹ To circumvent this difficulty, addition of a redox mediator, 2,2,6,6-tetramethylpiperidine 1-oxyl (TEMPO) was tried and FDCA was successfully produced in low pH conditions. However, the choice of electrolyte for electrolysis is important, in order to oxidise HMF into FDCA as well as support the long-term stability of HMF and electro-catalysts.³² With this perspective, finding an appropriate electrolyte that can stabilise both the electrode and the HMF is important for the electrochemical oxidation of HMF into FDCA.

In this manner, recently, metal boride or phosphorous have been implied frequently as an electrocatalysts on oxidation reaction, due to their noticeable reactivity in aqueous atmospheres.³³ To the best of knowledge, boride/phosphorous form of transition metal contributed on forming oxyhydroxide species under aqueous atmosphere, which shows catalytic activity and performance during electrochemical oxidation reaction.³⁴ Among various kinds of boride/phosphorous, especially, cobalt phosphorous (Co-P) has been widely applied for electrochemical reaction.^{35, 36} The formation of Co-P follows the net reaction for spontaneous reaction:³⁷



The Co-P deposited by pristine methods has limitations on durability, which the phosphorous is easily leaching out as the electrochemical reaction proceeds.³⁸

Therefore, following the results of a Co-P electrodes for HMF oxidation to FDCA reported by Jiang *et al.*,³⁹ we prepared two different kinds of Co-P electrodes. Co-P on copper foam fabricated by a modified potentiodynamic deposition method of Co species,⁴⁰ altering the reaction solvent to a DES and water. Subsequently, electrochemical oxidation of HMF to FDCA performed in lower pH (0.5 M NaHCO₃ solution at a pH of 12 to reduce HMF degradation during reaction. The reaction efficiency and the stability of the electrodes were compared in this study.

Experimental

Materials

Cobalt(II) sulfate heptahydrate (CoSO₄·7H₂O), sodium hypophosphite monohydrate (≥99%, NaH₂PO₂·H₂O), choline chloride (≥99%, (CH₃)₃N(Cl)CH₂CH₂OH), ethylene chloride, sodium bicarbonate (NaHCO₃), and potassium hydroxide were purchased from Aldrich and used as received. 5-hydroxymethylfurfural (HMF), 2-formyl-5-furancarboxylic acid (FFCA), 2,5-furandicarboxylic acid (FDCA), and 5-Hydroxy-methyl-2-furancarboxylic acid (HMFA) were purchased from Aldrich and used as received. 2,5-Diformylfuran (DFF) was purchased from TCI Chemical. Copper foam (CF) purchased from MTI Corporation. A Millipore Milli-Q Integral 10 System used for deionized water (18 MΩ/cm).

Preparation of ethaline as a deep eutectic solvent (DES)

Ethaline prepared by mixture of choline chloride and ethylene glycol (at a molar ratio of 1:2) at 357 K with stirring until a homogeneous colourless liquid formed.

Preparation of Co-P/CF (Co-P_H₂O)

CF (geometric area of 1 cm²) was thoroughly rinsed with water and ethanol to remove residual organic species before electrodeposition. Electrodeposition of Co-P_H₂O was performed using a three-electrode cell with an electrolyte composed of 50 mM CoCl₂·6H₂O and 0.1 M NaH₂PO₂·H₂O in water. CF, Pt wire, and Ag/AgCl (sat. A 4 M KCl) wire used as the working electrode, counter electrode, and reference electrode, respectively. Cyclic voltammetry (CV) for electrodeposition of Co-P_H₂O performed for 15 cycles, within the range -1.2 V to -0.3 V vs. Ag/AgCl reference electrode at a scan rate of 5 mV/s. After deposition, the samples were rinsed with methanol and deionised water.

Preparation of DES-stabilised Co-P/CF (Co-P_DES)

CF was rinsed using the same method described above. Electrodeposition of Co-P_DES was performed using the same methods as for Co-P_H₂O sample preparation, except that ethaline at 357 K was used as the electrolyte instead of water. Electrodeposition of Co-P_DES was performed for 15 cycles, within the range -1.0. to 0.1 V vs. Ag wire. After deposition, Co-P_DES was washed several times with water. The concentration of NaH₂PO₂·H₂O varied from 0.05 M to 0.2 M for comparison of Co-P_DES electrodes with different Co-P load amounts.

Characterisation

The surface morphologies of the prepared samples were investigated using field emission scanning electron microscopy (FE-SEM, Tescan, Mira 3) at an accelerating voltage of 20 kV. The atomic ratios of the samples were measured using an energy-dispersive X-ray spectrometer (EDS, Noran System Seven, Thermo Fischer) at an accelerating voltage of 5 kV. X-ray photoelectron spectroscopy (XPS, Kratos Axis Ultra) analysis was performed using an Al K-alpha source. The binding energies was calibrated by using the residual carbon 1s peak at 284.6 eV. Transmission electron microscopy (TEM, Zeiss Libra 200 FE) measurements were performed at 200 kV.

HMF stability test in different pH of solution

To evaluating HMF stability in different pH of solution, 1.0 M KOH solution (pH 13.6) and 0.5 M NaHCO₃ solution (pH 12) was prepared. The 5 mM of HMF dissolved in each solutions and solution stirred gently at the room temperature. The 10 μL of solution taken from solution in every 2 h and analysed using high-performance liquid chromatography. The concentration of remained HMF was calculated and plotted by using standard calibration curves.

Electrochemical HMF oxidation and product analysis

To investigate the catalytic abilities of both Co-P_H₂O and Co-P_DES, linear sweep voltammetry (LSV) was measured under

with and without HMF conditions. The electrochemical cell consisted of a three-electrode system with undivided cell (prepared samples for the working electrode, Pt wire for the counter electrode, and Ag/AgCl (4M KCl) electrode for the reference electrode) were used. The applied potential controlled by a potentiostat/galvanostat (VSP, Biologics). A 0.5 M NaHCO₃ solution (pH 12) with or without 5 mM HMF were used as the electrolyte, which purged with N₂ prior to use, to remove dissolved oxygen. The potential was swept from the open-circuit potential (V_{oc}) to the positive direction at 10 mV/s with stirring. The measurement results plotted against the reversible hydrogen electrode (RHE) using the equation:

$$E (V \text{ vs. RHE}) = E_0 (V \text{ vs. Ag/AgCl}) + 0.197 V + 0.059 \times \text{pH}$$

This allows facile comparison of the data against the thermodynamic water oxidation potential under the pH conditions used in this study. The geometric area of the working electrode used for calculating all current densities reported in this study.

For quantification of oxidation products, including yield and Faraday efficiency (FE), electrochemical HMF oxidation performed while applying a constant potential until 50 C of charge passed. The FE of FDCA product was calculated as follow:

$$\text{FE (\%)} = \frac{\text{mol of FDCA produced}}{\frac{\text{mol of total electrons passed}}{6}} \times 100 \%$$

For the electrochemical oxidation, a three-electrode system was used in which Co-P electrodes were used as the working electrode, Pt wire was used as the counter electrode and Ag/AgCl (4 M KCl) was used as the reference electrode, respectively, and 1.45 V vs. RHE of potential were applied. A 0.5 M sodium bicarbonate solution (pH 12) used as the electrolyte with 5 mM HMF. 10 μL of solution were taken from the cell during and after reaction, and analysed using high-performance liquid chromatography (HPLC, YL 9100, Younglin Instrument Ltd.) with a 265 nm wavelength set ultraviolet-visible detector. Sulfuric acid (5 mM) used as the mobile phase in isocratic mode, with a 0.5 mL/min flow rate at 338 K, was injected into the Hi-Plex H column. The quantification and qualification of products were performed by calibration curves (correlation coefficient = 0.999) by applying a standard solution of known concentration. All presented data are an average of triplicate experiments. The produced FDCA was confirmed by nuclear magnetic resonance spectroscopy (NMR, Bruker AVANCE III).

Results and discussion

Previous studies on the oxidation of HMF to FDCA have been performed under strong basic conditions because this activates the 5-position alcohol and oxidises the 2-position aldehyde group to produce FDCA, which has carboxyl groups at the 2- and 5-positions of the furan ring. However, excessive bases initiates nucleophilic attack for condensation reactions between HMF molecules, forming linkages at the alpha position or substitutions at the beta position of HMF, resulting in degradation and denaturation of HMF.^{41, 42}

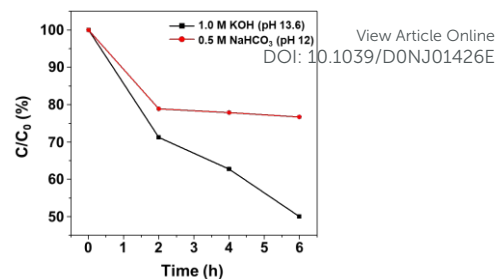


Fig. 1. Concentration change of HMF in two electrolytes with different pH conditions over time.

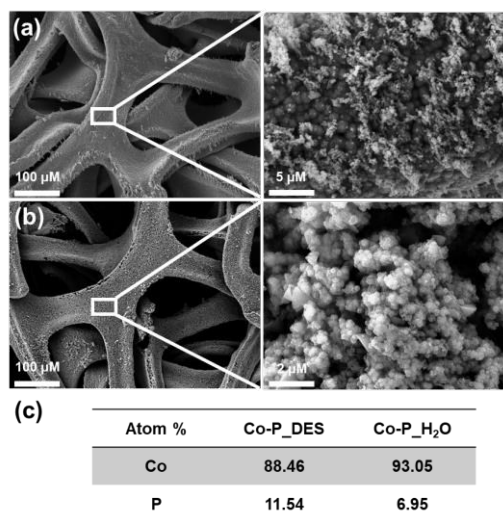


Fig. 2. SEM image of (a) Co-P_DES and (b) Co-P_H₂O electrodes; (c) table of SEM-EDS elemental analysis of Co and P.

As shown in Fig. 1, under the high pH condition of 1.0 M KOH (pH 13.6), HMF degrades quickly and only 50% of the initial concentration remains after 6h. Using 0.5 M NaHCO₃ electrolyte (pH 12) does not completely prevent HMF from degradation, but almost 80% of HMF still remains in solution. Thus, in this work, we used 0.5 M NaHCO₃ (pH 12) solution as the electrolyte during electrochemical HMF oxidation into FDCA.

Co-P_DES and Co-P_H₂O prepared by an electrodeposition method by cycling the designated potential ranges for 15 cycles. The CV curves during Co-P deposition in DES and H₂O shown in Fig. S1. As the reaction media changed for electrochemical deposition of Co-P on Cu foam, the morphology of the deposited Co-P showed noticeable changes, as shown in Fig. 2. Using Co-P_DES, more fine particles attached to the surface of the Cu foam, while with Co-P_H₂O, highly aggregated irregular particles attached to the Cu foam. Furthermore, SEM-EDS analysis results show that a higher amount of phosphorous is loaded when the electrodeposition of Co-P on CF is in DES rather than in H₂O (Fig. 2c).

The higher amount of loaded P in Co-P_DES also led to enhanced electrochemical efficiency of the HMF oxidation reaction, as shown by the LSV curves of different concentrations of P precursors (Fig. S2).

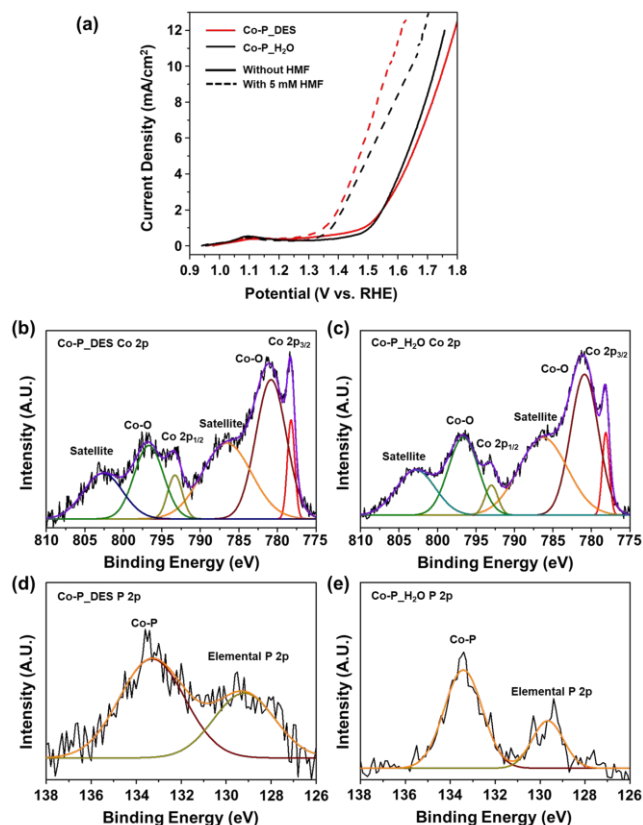


Fig. 3. (a) LSV curves of Co-P_DES and Co-P_H₂O, XPS Co 2p spectra of (b) Co-P_DES, (c) Co-P_H₂O, XPS P 2p spectra of (d) Co-P_DES, and (e) Co-P_H₂O

As the P precursor concentration increased, the onset potential (V_{onset}) shifted to a lower potential. Finally, the electrode deposited at 0.2 M P precursor showed the same V_{onset} of the metallic Co electrode. Accordingly, further experiments performed using electrodes deposited using 0.2 M P precursor. The optimal thickness of deposited Co-P layer investigated by scanning LSV curves depends on deposition cycles, which presented in Fig. S3. The 15 times of deposition cycles showed the best electrochemical catalytic properties of Co-P_DES electrode.

LSV curves of the as-deposited Co-P_DES and Co-P_H₂O electrodes shown in Fig. 3a. The solid line corresponds to the absence of HMF and the dashed line corresponds to its presence at 5 mM concentration in 0.5 M NaHCO₃ electrolyte. The V_{onset} of the solid line is the initiation potential for water oxidation, which was 1.5 V vs. RHE for Co-P_DES and 1.53 V vs. RHE for Co-P_H₂O electrode.

However, when 5 mM HMF was added (dashed line), the V_{onset} shifted to 1.34 V vs. RHE for Co-P_DES and 1.37 V vs. RHE for the Co-P_H₂O electrode, indicating that where Co-P deposited in DES solvent showed a lower V_{onset} than that in H₂O solvent.

The surface-deposited Co-P composition of both electrodes investigated by X-ray photoelectron spectroscopy (XPS). Fig. 3b and c show the Co 2p spectra of Co-P_DES and Co-P_H₂O, respectively.

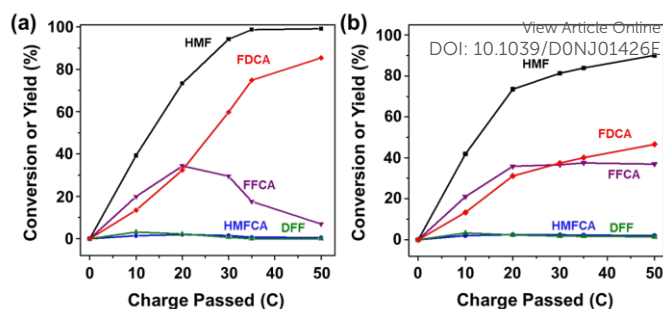


Fig. 4. HMF conversion and product yield curves vs. charge passed for (a) Co-P_DES and (b) Co-P_H₂O electrodes

Six kinds of peaks are observed for both electrodes, which correspond to Co 2p_{3/2} (778.2 eV), Co-O (780.8 eV), satellite (786.6 eV), Co 2p_{1/2} (793.3 eV), Co-O (796.7 eV), and satellite (802.8 eV), respectively.²⁶ In the case of the P 2p spectra, elemental P (129.7 eV) and P from Co-P (133.2 eV) are observed in both Co-P_DES (Fig. 3 d) and Co-P_H₂O (Fig. 3 e), respectively.⁴³

The Co 2p and P 2p XPS spectra of Co-P_DES and Co-P_H₂O are consistent with previously reported results for Co-P, which means that Co-P is well deposited on CF using either solvent usage.⁴⁴ However, a higher phosphorous ratio in Co-P_DES led to a more distinct peak of larger intensity for the P 2p spectrum compared to that of Co-P_H₂O, which agrees well with the above SEM-EDS analysis results.

According to the LSV results presented in Fig. 3a, 1.45 V vs. RHE is the optimal potential for both electrodes, which favours the HMF oxidation reaction over the water oxidation reaction.

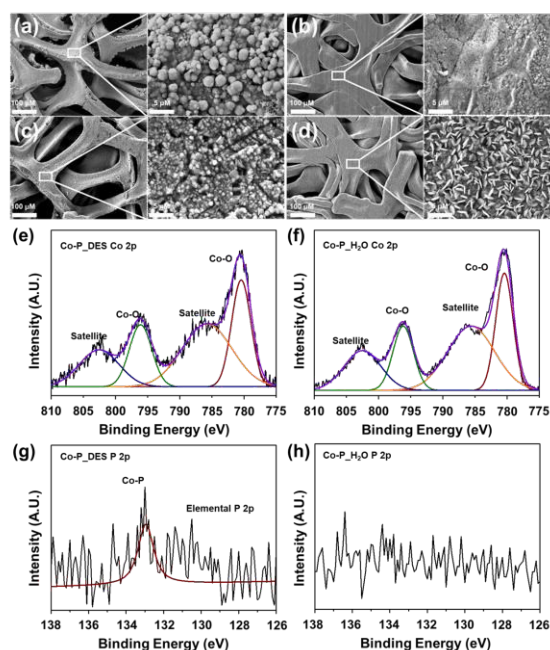


Fig. 5. SEM images of Co-P_DES (a) before reaction and (b) after reaction, SEM images of Co-P_H₂O (c) before reaction and (d) after reaction, XPS Co 2p spectra of (e) Co-P_DES and (f) Co-P_H₂O after HMF oxidation reaction, P 2p spectra of (g) Co-P_DES, and (h) Co-P_H₂O after HMF oxidation reaction.

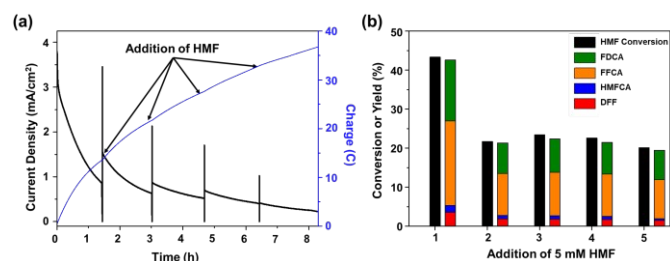


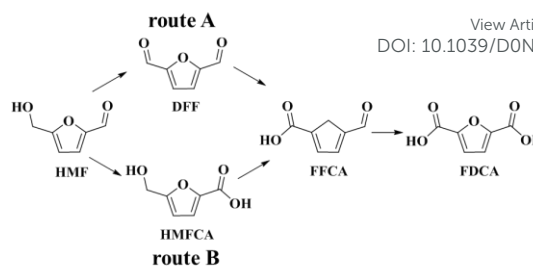
Fig. 6. (a) *j*-*t* plot with passed charge of Co-P_DES with repeated reaction cycles, (b) HMF conversion and Product yield profile as repeated addition of 5 mM fresh HMF.

Thus, the conversion of HMF by both Co-P_DES and Co-P_H₂O electrodes was performed using 0.5 M NaHCO₃ electrolyte at 1.45 V vs. RHE, with a total charge of 50 C, and the reaction product was analysed every 10 C of charge.

At the initial stage of the reaction (<20 C), FFCA was produced as the major product of the reaction with both Co-P_DES and Co-P_H₂O electrodes. However, after 20 C, the yield of FDCA increased. After 50 C, the FFCA yield decreased and 85.3% yield of FDCA was obtained with 99% of HMF conversion, and the Faraday efficiency of HMF conversion to FDCA was 77.3% using the Co-P_DES electrode (Fig. 4a). The detailed *j*-*t* curves during HMF oxidation reaction by Co-P_DES and Co-P_H₂O presented on Fig. S4. In the case of the Co-P_H₂O electrode, a slight increase in the FDCA yield observed, while the FFCA yield maintained during the whole reaction, and a 46.5% yield of FDCA obtained with 89.9% of HMF conversion. The Faraday efficiency of HMF to FDCA conversion was 41.4% (Fig. 4b). It is notable that the yield of HMFCFA and DFF was less than 3% for both the Co-P_DES and Co-P_H₂O electrodes.

The produced FDCA was purified and confirmed by NMR spectroscopy. The two peaks was observed which first one is from aromatic singlet protons (denoted as H_A) and the other is from hydroxyl protons (denoted as H_B), with chemical shifts of 7.3 ppm and 13.6 ppm, respectively (Fig. S5). The measured NMR spectrum was in a good accordance with previously reported NMR spectrum of FDCA.⁴⁵

To determine the reason why different FDCA yields observed even when they were both Co-P deposited Cu foam electrodes, SEM images of each electrode after the reaction were analysed. In the image of the Co-P_DES electrode after the reaction, surface-attached Co-P particles are pulverised into smaller particles, maintaining the original shape of Co-P (Fig. 5 a and b). Conversely, in the case of the Co-P_H₂O electrode, the morphology of the particles dramatically changed from a round-type particle to a hexagonal plate shape, which proves that the surface-deposited Co-P changed into cobalt oxides or oxyhydroxides (Fig. 5 c and d). To reveal the changed surface state of both electrodes after the HMF oxidation reaction, Co 2p and P 2p XPS analyses performed. Both the metallic Co 2p_{1/2} and Co 2p_{3/2} peaks (binding energies of 793.3 and 778.2 eV, respectively) disappear for Co-P_DES and Co-P_H₂O after reaction. Only Co-O peaks (796.7 eV and 780.8 eV) and their satellite peaks (786.8 eV and 802.8 eV) observed (Fig. 5 e and f). However, in the case of the P 2p spectra of both electrodes,



Scheme 1. Possible pathways of electrochemical HMF oxidation into FDCA

a small P peak for the Co-P (133.2 eV) is observed only for the Co-P_DES electrode, while no phosphorous peak is observed for the Co-P_H₂O electrode (Fig. 5g and h). To obtain more information on the catalytic activity of Co-P_DES for the electrochemical HMF oxidation reaction, a repeated reaction at 1.45 V vs. RHE with 5 mM HMF addition was performed.

The Co-P_DES showed electrocatalytic properties until fourth times of repeated continuous reaction (Fig. 6a). The HMF conversion and product yield profile as repeated addition of 5 mM of fresh HMF (Fig. 6b). As repeated reaction cycle increases, distribution of HMF oxidation products was maintained, which means that Co-P_DES electrode is stable, with in a good accordance with above XPS analysis results.

The electrochemical oxidation of HMF into FDCA follows the two pathway which shown as Scheme 1. The first pathway is HMF oxidize into 2,5-Furandicarboxaldehyde (DFF) (route A). The other pathway is HMF oxidize into 5-hydroxymethyl-2-furancarboxylic acid (HMFCFA) (route B). Both pathways are converge into 5-formyl-2-furancarboxylic acid (FFCA) and FDCA obtained as final product. Under the base condition, HMF rapidly converted into HMFCFA by nucleophilic addition of hydroxide ion, forming a geminal diol and then, proton transfer from water to the intermediate of alkoxy ion forms FFCA.¹⁴

According to the above analysis results, the decreased efficiency of Co-P_DES and Co-P_H₂O electrodes derived from a loss of phosphorous atoms during the reaction, converting surface-attached Co-P particles into cobalt oxides. Since the hydrogen evolution reaction occurs as by-reaction during preparation of Co-P_H₂O, stability of surface electrodeposited Co-P decreases in H₂O atmosphere. Additionally, DES have typical properties such as good ionic conductivity and good solubility of metal salts, and do not degrade products. In these reasons, Co-P synthesised in DES shows better electrochemical properties.⁴⁶

Conclusions

In summary, electrodeposited Co-P on Cu foam in different solvents of water and DES, and these applied as electrodes for the electrochemical HMF oxidation reaction to FDCA. The Co-P synthesised in DES solvent showed 99% HMF conversion with 85.3% FDCA yield, a remarkably increased performance compared with Co-P synthesised under H₂O as the reaction solvent, also demonstrated long-term stability. Referring to the previously reported advantages of DES as a reaction solvent

ARTICLE

Journal Name

such as good ionic conductivity, easily prepared, nontoxic, low-cost, and biodegradable, this work shows that DES also contributes to the stability of synthesised metal-phosphorous-based electrodes. Thus, this work suggests the usability of DES to replace water as a reaction solvent for preparing electrodes by electrodeposition, with enhanced sustainability and better efficiency of electrodes.

Conflicts of interest

There are no conflicts to declare.

Acknowledgements

This work was supported by Basic Science Research Program (NRF-2019R1C1C1004210) and (NRF-2019R1F1A1058695) through the National Research Foundation of Korea (NRF) grant funded by the Ministry of Science, ICT and Korea Research Institute of Chemical Technology (KRICT) core project (SS2042-10).

Notes and references

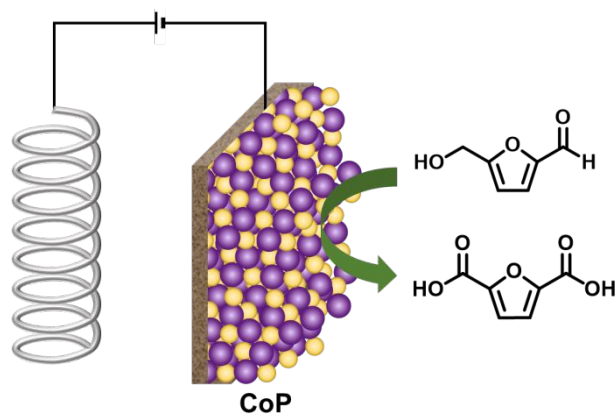
1. A. P. Abbott, G. Capper, D. L. Davies, H. L. Munro, R. K. Rasheed and V. Tambyrajah, *Chem. Comm.*, 2001, 2010-2011.
2. A. P. Abbott, G. Capper, D. L. Davies, R. K. Rasheed and V. Tambyrajah, *Chem. Comm.*, 2003, 70-71.
3. A. P. Abbott, D. Boothby, G. Capper, D. L. Davies and R. K. Rasheed, *J. Am. Chem. Soc.*, 2004, **126**, 9142-9147.
4. N. M. Pereira, C. M. Pereira, J. P. Araújo and A. Fernando Silva, *J. Electroanal. Chem.*, 2017, **801**, 545-551.
5. A. P. Abbott, J. C. Barron, G. Frisch, K. S. Ryder and A. F. Silva, *Electrochim. Acta*, 2011, **56**, 5272-5279.
6. X. Cao, L. Xu, Y. Shi, Y. Wang and X. Xue, *Electrochim. Acta*, 2019, **295**, 550-557.
7. X.-J. Shen, J.-L. Wen, Q.-Q. Mei, X. Chen, D. Sun, T.-Q. Yuan and R.-C. Sun, *Green Chem.*, 2019, **21**, 275-283.
8. B. L. Kuhn, G. C. Paveglia, S. Silvestri, E. I. Muller, M. S. P. Enders, M. A. P. Martins, N. Zanatta, H. G. Bonaccorso, C. Radke and C. P. Frizzo, *New J. Chem.*, 2019, **43**, 1415-1423.
9. M. R. S. J. Foreman, S. Holgersson, C. McPhee and M. S. Tyumentsev, *New J. Chem.*, 2018, **42**, 2006-2012.
10. W. Yu, C. Wang, Y. Yi, W. Zhou, H. Wang, Y. Yang and Z. Tan, *Cellulose*, 2019, **26**, 3069-3082.
11. D. E. Crawford, L. A. Wright, S. L. James and A. P. Abbott, *Chem. Comm.*, 2016, **52**, 4215-4218.
12. P. McKendry, *Bioresour. Technol.*, 2002, **83**, 37-46.
13. M. Parikka, *Biomass Bioenerg.*, 2004, **27**, 613-620.
14. H. Yu, K.-A. Kim, M. J. Kang, S. Y. Hwang and H. G. Cha, *ACS Sustainable Chem. Eng.*, 2019, **7**, 3742-3748.
15. T. W. G. Petersen, *Top Value Added Chemicals from Biomass: Volume 1—Results of Screening for Potential Candidates from Sugars and Synthesis Gas*, Report DOE/GO-102004-1992, National Renewable Energy Laboratory, 2004, 26-28.
16. P. Sharma, M. Solanki and R. K. Sharma, *New J. Chem.*, 2019, **43**, 10601-10609.
17. X. Han, C. Li, Y. Guo, X. Liu, Y. Zhang and Y. Wang, *Appl. Catal. A*, 2016, **526**, 1-8. DOI: 10.1039/D0NJ01426E
18. S. R. Kubota and K.-S. Choi, *ChemSusChem*, 2018, **11**, 2138-2145.
19. B. J. Taitt, D.-H. Nam and K.-S. Choi, *ACS Catal.*, 2019, **9**, 660-670.
20. N.-T. Suen, S.-F. Hung, Q. Quan, N. Zhang, Y.-J. Xu and H. M. Chen, *Chem. Soc. Rev.*, 2017, **46**, 337-365.
21. L. Gao, Y. Bao, S. Gan, Z. Sun, Z. Song, D. Han, F. Li and L. Niu, *ChemSusChem*, 2018, **11**, 2547-2553.
22. W.-J. Liu, L. Dang, Z. Xu, H.-Q. Yu, S. Jin and G. W. Huber, *ACS Catal.*, 2018, **8**, 5533-5541.
23. H. Chen, J. Wang, Y. Yao, Z. Zhang, Z. Yang, J. Li, K. Chen, X. Lu, P. Ouyang and J. Fu, *ChemElectroChem*, 2019, **6**, 5797-5801.
24. D.-H. Nam, B. J. Taitt and K.-S. Choi, *ACS Catal.*, 2018, **8**, 1197-1206.
25. Z. Zhou, C. Chen, M. Gao, B. Xia and J. Zhang, *Green Chem.*, 2019, **21**, 6699-6706.
26. M. J. Kang, H. Park, J. Jegal, S. Y. Hwang, Y. S. Kang and H. G. Cha, *Appl. Catal. B*, 2019, **242**, 85-91.
27. X. Huang, J. Song, M. Hua, Z. Xie, S. Liu, T. Wu, G. Yang and B. Han, *Green Chem.*, 2020, **22**, 843-849.
28. H. M. Pham, M. J. Kang, K.-A. Kim, C. G. Im, S. Y. Hwang and H. G. Cha, *Korean J. Chem. Eng.*, 2020, **37**, 556-562.
29. L. Gao, Z. Liu, J. Ma, L. Zhong, Z. Song, J. Xu, S. Gan, D. Han and L. Niu, *Appl. Catal. B*, 2020, **261**, 118235.
30. M. Sajid, X. Zhao and D. Liu, *Green Chem.*, 2018, **20**, 5427-5453.
31. K. R. Vuyyuru and P. Strasser, *Catal.*, 2012, **195**, 144-154.
32. H. G. Cha and K.-S. Choi, *Nat. Chem.*, 2015, **7**, 328-333.
33. S. Barwe, J. Weidner, S. Cychy, D. M. Morales, S. Dieckhöfer, D. Hiltrop, J. Masa, M. Muhler and W. Schuhmann, *Angew. Chem. Int. Ed.*, 2018, **57**, 11460-11464.
34. D. K. Zhong and D. R. Gamelin, *J. Am. Chem. Soc.*, 2010, **132**, 4202-4207.
35. M. W. Kanan and D. G. Nocera, *Science*, 2008, **321**, 1072-1075.
36. K. W. Cho and H. S. Kwon, *Catal. Today*, 2007, **120**, 298-304.
37. F. H. Saadi, A. I. Carim, E. Verlage, J. C. Hemminger, N. S. Lewis and M. P. Soriaga, *J. Phys. Chem. C*, 2014, **118**, 29294-29300.
38. W. Li, X. Gao, D. Xiong, F. Xia, J. Liu, W.-G. Song, J. Xu, S. M. Thalluri, M. F. Cerqueira, X. Fu and L. Liu, *Chem. Sci.*, 2017, **8**, 2952-2958.
39. N. Jiang, B. You, R. Boonstra, I. M. Terrero Rodriguez and Y. Sun, *ACS Energy Lett.*, 2016, **1**, 386-390.
40. R. Hallaj, K. Akhtari, A. Salimi and S. Soltanian, *Appl. Surf. Sci.*, 2013, **276**, 512-520.
41. G. Tsilomelekis, M. J. Orella, Z. Lin, Z. Cheng, W. Zheng, V. Nikolakis and D. G. Vlachos, *Green Chem.*, 2016, **18**, 1983-1993.
42. H. Ait Rass, N. Essayem and M. Besson, *ChemSusChem*, 2015, **8**, 1206-1217.
43. H. Jung and A. Alfantazi, *Electrochim. Acta*, 2006, **51**, 1806-1814.
44. X.-y. Yan, S. Devaramani, J. Chen, D.-I. Shan, D.-d. Qin, Q. Ma and X.-q. Lu, *New J. Chem.*, 2017, **41**, 2436-2442.
45. X. Han, L. Geng, Y. Guo, R. Jia, X. Liu, Y. Zhang and Y. Wang, *Green Chemistry*, 2016, **18**, 1597-1604.
46. A. A. C. Alcanfor, L. P. M. dos Santos, D. F. Dias, A. N. Correia and P. de Lima-Neto, *Electrochim. Acta*, 2017, **235**, 553-560.

Table of Contents Entry

**Deep Eutectic Solvent Stabilised Co-P film for
Electrocatalytic Oxidation of 5-hydroxymethylfurfural into
2,5-furandicarboxylic Acid**Myung Jong Kang,^a Hye Jin Yu,^{a,b} Hyun Sung Kim^{b,*} and Hyun Gil Cha^{a,*}^a Center for Bio-based chemistry, Korea Research Institute of Chemical Technology (KRICT), Ulsan
44429, Republic of Korea^b Department of Chemistry, Pukyong National University, Busan 48513, Republic of Korea

hgcha@kRICT.re.kr

1
2
3
4
5
6
7
8
9
10
11
12
13
14
15
16
17
18
19
20
21
22
23
24
25
26
27
28
29
30
31
32
33
34
35
36
37
38
39
40
41
42
43
44
45
46
47
48
49
50
51
52
53
54
55
56
57
58
59
60



The Co-P electrode synthesized in deep eutectic solution showed enhanced stability for electrocatalytic HMF oxidation into FDCA.